3D Modelling of Iron Sand Using Geoelectrical Resistivity Method with Wenner Array in Ulakan Tapakis, Padang Pariaman, West Sumatra

3D Modelling of Iron Sand Using Geoelectrical Resistivity Method with Wenner Array in Ulakan Tapakis, Padang Pariaman, West Sumatra

Adree Octova[1,4,*], Yoszi Mingsi Anaperta[1,4], Helio Gina Febriandika[1], Herry Martinus[2], Admizal Nazki[2,3], Pakhrur Razi[4,5], Amali Putra[5]

[1]Department of Mining Engineering, Faculty of Engineering, Universitas Negeri Padang, Jl. Prof. Hamka, Padang 25131, Indonesia
[2]Department of Energy and Mineral Resources of West Sumatra Province, Jl. Joni Anwar No.85, Kp. Lapai, Nanggalo, Padang 25142, Indonesia.
[3]Doctoral Program of Environmental science, Universitas Negeri Padang, Jl. Prof Hamka, Padang 25131, Indonesia
[4]Center of Disaster Monitoring and Earth Observation Physics Department Universitas Negeri Padang, Jl. Prof Hamka, Padang 25131, Indonesia
[5]Department of Physics, Faculty of Mathematics and Natural Science, Universitas Negeri Padang, Jl. Prof Hamka No. 121, Padang 25131, Indonesia

*adree@ft.unp.ac.id

Abstract. A studies using the resistivity method have been carried out to determine the potential of iron sand in Ulakan Tapakis West Sumatra. This study aims to establish the potential 3D modelling of iron sand. Wenner array is used to determine location of anomalies by taking 5 sections which has 180 meter length. The distance of the electrode used is 3.9 meters. Generally, Ulakan Tapakis has 3 main components of alluvial deposits, namely a layer of top sand (upper sand), middle sand, and a layer of iron sand which is divided into 2 layers, namely the bottom sand and the iron sand layer which has a resistivity value ranging from 9.53 -14135 Ωm. These layers have different resistivity values depending on the constituent material. The existance of iron sand is located at depths of 0-6 meter below sea surface, with range of resistivity is 9.53-1000 Ωm.

1. Introduction

West sumatera is one of the provinces in the middle of Sumatera Island with the capital city of Padang. This province as we know has a fault caused by the movement of tectonic plate namely Indo Autralian and Eurasian Plate called the Great Sumatran Fault or also known as Semangko Fault that nowadays, the pressure on the fault has increased tremendously[1].

West Sumatra Province has complex physiographic conditions, namely: volcanic mountain areas, tertiary fold hills, and lowland areas. Potential metal minerals found in West Sumatra Province are gold, iron ore, iron sand, copper, manganese, lead or lead, and mercury.

One area that has the potential for iron sand on the west coast of West Sumatra is the Ulakan Beach area, Padang Pariaman. This is evidenced by previous research on other beaches around Ulakan Beach. As has been done by the following researchers who have conducted research in the areas of

Kinali, Pasaman, Kata Beach, Pariaman, Tiram Beach, Pariaman, Sunur Beach, Pariaman, Beach Pasia Paneh Tiku, Agam [2][3].

Based on data from the Padang Pariaman Regency government, there is iron sand in the Ulakan and Sanur Beach areas with a ready-to-mine area of 2000 m^2. However, research activities in the Ulakan area have not been carried out to determine the potential of iron sand in the area itself. Therefore, to find out the description and presence of iron sand, it is necessary to conduct a wider research through geophysical exploration activities. The research was conducted using the geoelectric method by measuring the resistivity of sediments in coastal areas. So from the interpretation of the resistivity values, the distribution, lithology and quality of iron sand are obtained.

Geoelectrical resistivity method consists of several parts, one of which is resistivity or resistivity. The resistivity method is one of a group of geoelectrical methods used to study subsurface conditions by studying the nature of electric currents in rocks below the earth's surface.

Geoelectrical resistivity method is more effective if used for shallow exploration, rarely used to provide information on layers at a depth of more than 2 km.

2. Geoelectrical Resistivity Method

Geoelectrical is a method in geophysics that studies the nature of the flow of electricity in the earth. Detection above the surface includes the measurement of potential, current, and electromagnetic fields that occur both naturally and as a result of injecting currents into the earth. The working principle of the geoelectrical method is done by injecting an electric current into the ground through a pair of electrodes and measuring the potential difference with another pair of electrodes. When an electric current is injected into a medium and the potential difference (voltage) is measured, the resistance value of the medium can be estimated. Based on the research objectives, the method used is the mapping method. The resistivity mapping method is a resistivity method that aims to study variations in the resistivity of the subsurface horizontally [4].

The value of the resistivity below the surface is obtained from the injection of current and the difference in the value of the potential difference on the surface will be obtained. Schematic of current flow and potential field for homogeneous subsurface depicted in Figure 1 and Figure 2.

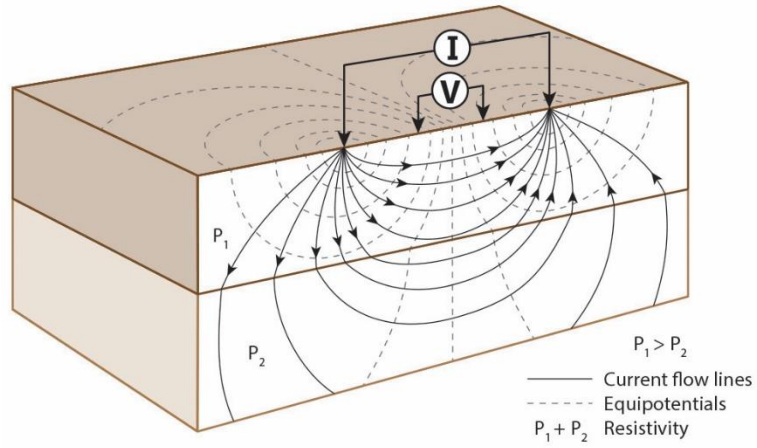

Figure 1. The shape of the electrode changes for the apparent resistivity measurement

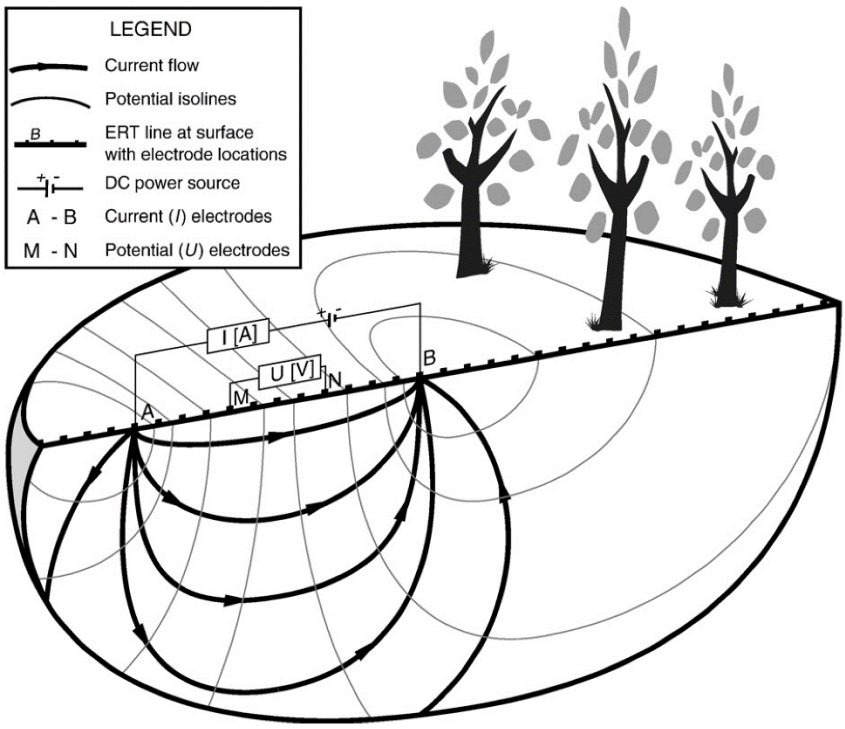

Figure 2. Schematic of a homogeneous subsurface current flow and potential field [4]

The geoelectrical resistivity method is based on the assumption that the earth has an isotropic homogeneous nature. With this assumption, the measured resistivity is the actual resistivity and does not depend on the electrode spacing. But in reality the earth is composed of layers with different resistivity, so the measured potential is the influence of these layers [5].

Therefore, the value of resistivity measured is as if it were the value of resistivity for one layer only. The measured resistivity is actually the apparent resistivity (ρa) [6]
The magnitude of the apparent resistivity (ρa) is:

$$\rho a = \frac{2\pi}{\left(\frac{1}{r1}-\frac{1}{r2}\right)-\left(\frac{1}{r3}-\frac{1}{r4}\right)} \text{ x } \frac{\Delta V}{I} \quad (1)$$

or

$$\rho a = K.\frac{\Delta V}{I} \quad (2)$$

with

$$K = \frac{2\pi}{\left(\frac{1}{r1}-\frac{1}{r2}\right)-\left(\frac{1}{r3}-\frac{1}{r4}\right)} \quad (3)$$

Where K is the geometric factor, namely: the magnitude of the correction for the location of the two potential electrodes to the current electrode location. By measuringΔV and I then can determine the value of the resistivity [6].

The price of rock resistivity depends on the various materials, density, porosity, size and shape of rock pores, water content, and quality and temperature [7][8][9][10]. Thus there is no certainty of the value of resistivity for each type of rock in the aquifer consisting of loose material.
In general, based on resistivity values, rocks and minerals can be grouped into three, namely:

- Good conductor : $10^{-8} < \rho < 1$ Ωm
- Intermediate conductor : $1 < \rho < 10^{7}$Ωm
- Isolators: $\rho > 10^{7}$ Ωm

Table 1. The resistivity value of geological materials [7]

Material	Specific resistance value (Ωm)
Iron	$5 \times 10^{-7} - 10$
Silt	30-215
Sand and gravel	30-225
Gravel	1400
Quartz SiO2	3×10^{2}-106
Hematite Fe203	3.5×10^{-3}-10^{7}
Limonite Fe203.nH20	10^{3}-10^{7}
Magnetite FeO, Fe203	5×10^{-5}-5.7×10^{2}
Ilmenite FeTi03	10^{-3}-5 x 10
Bauxite Al2O3	$10^{-7} - 2 \times 10^{-3}$
Dolomite MgO	3.5×10^{2}-5×10^{3}
Pyrite FeS2	2.9×10^{-5}-1.5
Chalcopyrite	1.2×10^{-5} - 3×10^{-1}
Pyrotite FeI-xS	7.5×10^{-6}-5×10^{-2}
Galena PbS2	3×10^{-5}-3×10^{2}
Water H2O	30 – 100

2.1. Wernner Array

This method was introduced by Wenner (1915). System array in geoelectrical exploration with the arrangement of equal spacing (r1 = r4 = a and r2 = r3 = 2a). The distance between the current electrodes is three times the potential electrode distance, the potential distance from the sounding point is a/2, so the distance between each current electrode and the sounding point is 3a/2. The target depth that can be achieved in this method is a/2. In field data acquisition, the arrangement of current and potential electrodes is placed symmetrically with the sounding point [11].

In the Wenner array, the distance between the current electrode and the potential electrode is the same. As shown in the picture (Figure 3)

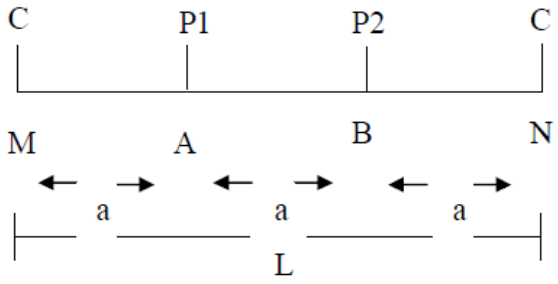

Figure 3. Current and potential electrodes in the Wenner array [12]

From the picture above, it can be seen that the distance AM = NB = a and the distance AN = MB = 2a, using the equation:

$$K = \frac{2\pi}{\left(\frac{1}{a}-\frac{1}{2a}\right)-\left(\frac{1}{2a}-\frac{1}{a}\right)} \quad (4)$$

$$K = 2\pi a \quad (5)$$

3. Research Area

Based on geological maps by Kastowo et al, 1996, the rock formations found in Padang Pariaman Regency are generally formed during the quarter consisting of surface deposits (Qal), volcanic volcanic rocks (Qhpt, Qpt, Qtau) that are decomposed and intrusive rocks formed at Middle Miocene Tertiary (Tmgr).

The rock is dominated by alluvial deposits (Qal) in the form of silt, sand and gravel found on the coastal plain, including swamp deposits in the southwest of Lubuk Alung and there are remnants of pumice (Qhpt or Qpt).

Then there are pumice and andesite tuff rocks (Qpt) consisting of glass fibers containing almost no mafic minerals with a diameter of 1-20 cm and rather compact. In the surrounding area there is a layer of sand that is rich in quartz, obsidian and pitchstone minerals. This tuff deposit is thought to have originated from the recent erosion of the Maninjau caldera or the fissure eruption associated with the Sumatran fault line [13]. Andesitic rock assemblages consisting of undivided flows, lahars, fangglomerates and other collovial deposits are derived from strato-cone volcanoes and are less eroded. Its age is estimated to be Pleistocene to Holocene.

The area around the reed river has hardened crystal tuff (QTt) well, pink in color and composed of a matrix rich in glass fibers with quartz, plagioclase and volcanic fragments of intermediate to acidic composition with a diameter of almost 10 cm.

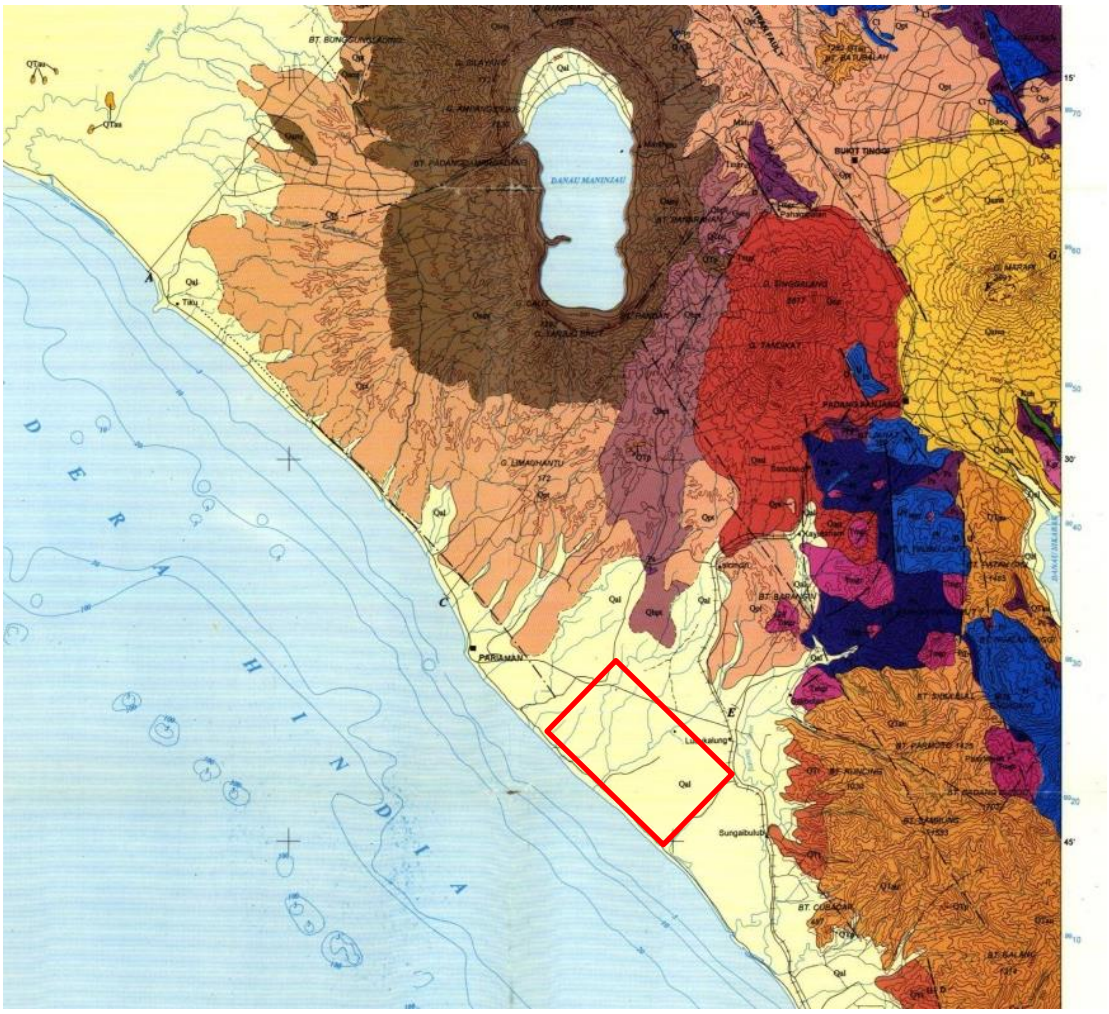

Figure 4. Geological Map of Padang Pariaman Regency (taken from the geological map of the field sheet by Kastowo, et al. 1996). The red line is the research area, Ulakan Tapakis

Miocene granitic rock of tertiary age (Tmgr) stockists composed of granite and quartz diorite are found in the foothill areas around Sicincin and Padang Panjang which are pyritated and eroded indicating significant hydrothermal changes in these stocks.

Based on the geological map, the iron sand found in the coastal area of Padang Pariaman was formed as a result of weathered transportation of acidic igneous rocks containing iron (Fe) which accumulated through rivers from the Maninjau Lake caldera, Singgalang Mountain and Tandikek Mountain, one of whose downstream is located at Ulakan Tapakis area

Rocks of land origin that are mechanically eroded form a supply of clay to sand-sized materials containing heavy minerals containing iron (Fe) such as magnetite, titanomagnetite and ilminite to river flows that are deposited on the coast.

When the mechanical weathering process occurs, all the original rock material enters the sea, where the movement of water sifts the material into several components, each of which is sedimented in several areas around the coast. The sand being the largest is transported by waves towards the coast where it may be deposited at the top of the beach. Silt and clay may remain in the coastal zone for a while but slowly move into the deep sea (Figure 4)

4. Method

The designed of geoelectrical section measurement design with a section distance of 55 – 65 m and a total section distance of 200 m, a section length of 180 m, totaling 5 lines. The direction of the geoelectrical trajectory extends southwest towards the northeast with an electrode distance of 3.9 m. As shown in Figure 5:

Figure 5. Sections Measurement

The following are the work steps that will be carried out when measuring the resistivity value of the research area:

1) Determine the measurement points to be carried out in the measurement area
2) Determine the electrode spacing to be made on the measurement path.
3) Measure the measurement path according to the predetermined path length and electrode spacing.
4) Embed electrodes at each electrode spacing that has been determined.
5) Connect the electrode cable to the section and connect the battery to the tool.
6) Activate the device and ensure that the battery is at least 85% charged
7) Calibrate the tool, then choose the available measurement method and its array, in this case the geoelectrical resistivity Mapping method with Wenner array
8) Taking measurements, the data obtained is directly stored on the Main Unit.

The data processing that the author does is the calculation method using software to produce 3 dimensional mapping data and then analyzes the data. Data obtained from the field, namely the value of resistivity, current strength and potential difference were processed to obtain apparent resistivity from the research location using Ms. Excel, and inputted into res2dinv software to obtain subsurface structure data in the form of sediment resistivity values. Furthermore, the data is processed with Surpac software to provide a 3d image of the subsurface layer so that the 3d mapping data of the research location is obtained to be interpreted and analyzed the results.

The 2D cross-section of the resistivity value describes the variation in the resistivity value of minerals in the subsurface layers of the earth in the form of different color images. The cross sections are then correlated to produce a 3D interpretation of iron sand deposits. The resistivity value obtained from the interpretation (apparent resistivity) is then compared with the value of the resistivity variation of the earth material (rock). The maximum depth achieved can be calculated based on the length of the measuring path.

After modeling, the inversion results are compared with the resistivity values obtained by processing data to ensure the correctness of the modeling results obtained.

5. Result and Discussion

Based on the geological map of Lembar Padang by Kastowo et al, 1996, the Ulakan Tapakis area is dominated by alluvial surface deposits that were formed during the Quaternary Holocene. It has a thickness around 1000 m, as well as constituent materials consisting of sand, gravel, silt found in coastal areas. The research area itself is not only used as an area for cultivation and collection of marine products, there are also livestock such as cows, goats and chickens. This causes the sedimentary material there to be mixed with livestock waste so that the resistivity value in the study area has a very high range.

Thus, based on the constituent materials and the value of the resistivity of the material [7], the sediment lithology of the study area is classified into 4 types, namely sand deposits containing other materials such as organic material, named upper sand layer, containing gravel (middle sand layer), a layer containing silt material with indications of iron sand with a higher resistivity value (bottom sand layer), and a layer of iron sand with a low resistivity value (iron sand layer). Each of these layers is shown in sequence in red-purple, yellow-orange, green (dark-light), and blue (dark-young).

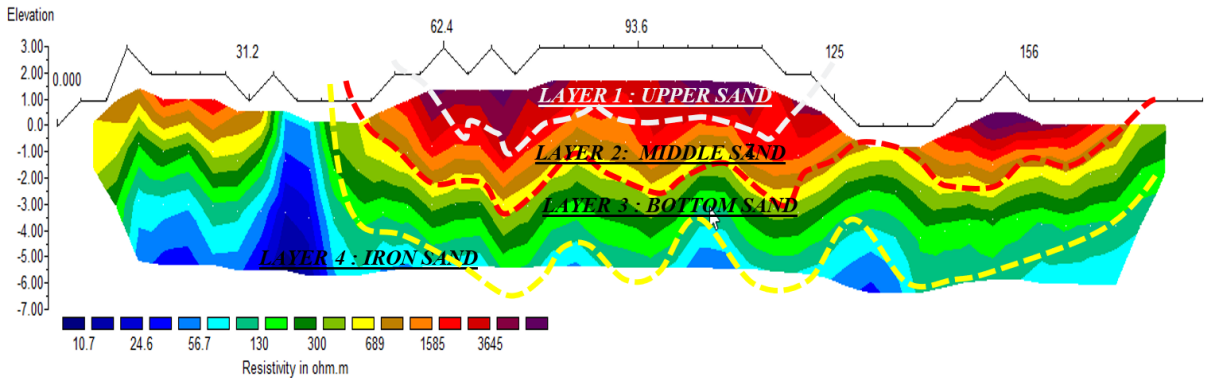

Figure 6. Resisitivity Inversion With Topography Data in Section 1

In the Figure 6, the range of sediment resistivity values in the Ulakan area is 10.7-3645 Ω m, it can be seen that the dominant iron sand carrier layer is seen in layer 4 with a dark blue layer followed by a light blue to green layer (bottom sand) with the resistivity value is 10.7 – 450 Ω m. At electrodes 9 – 11 with a distance of 35.1 - 42.9 m from electrode 1, there is an outcrop of iron sand, which is estimated to be up to a depth about 6 m, but at the time of data collection, the outcrop is not visible, this is caused by section area covered by grass.

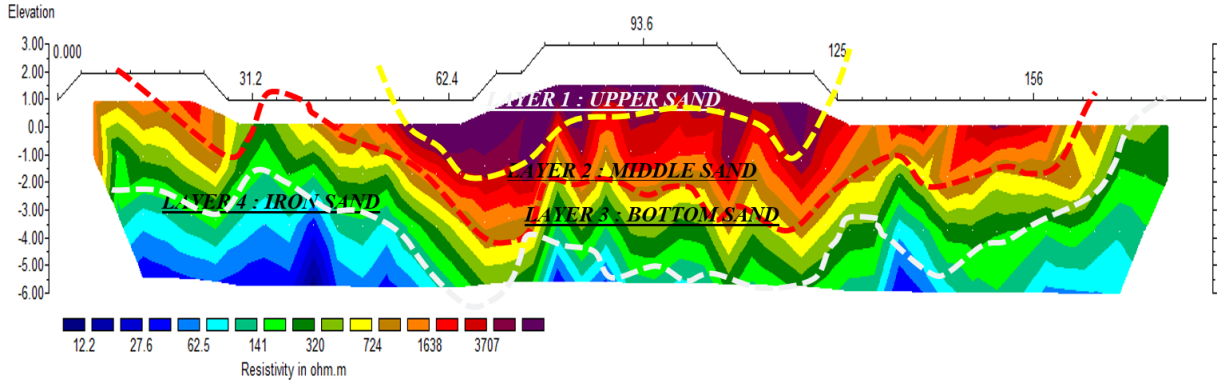

Figure 7. Resisitivity Inversion With Topography Data in Section 2

The range of resistivity values of section 2 (Figure 7) is 12.2 – 3707 Ω m which consists of 4 layers of sand consisting of the top, middle, bottom and iron sand layers.

The upper sand layer has more organic material than section 1, with a little sand content so that the specific resistance value is higher than the upper sand layer 1, which is more than 1638 Ω m. The thickness of this layer is around 1-2 m, but the average is 1 m.

The second layer of sand (middle sand) is thicker than the upper sand layer, a more even distribution forming a more even thickness, which is about 2 m. The resistivity value ranges from 520 – 1638 Ω m. Indicated by a white-yellow line.

The iron sand layer can be seen in areas that are dark blue to green. The green layer (bottom sand) is sand that has a higher resistivity of iron minerals than the blue layer (iron sand). The iron sand layer in section 2 has an estimated average thickness of 2 m, found at a depth of 3.5 - 6 m with a higher resistivity value than the iron sand in section 1 of 12.2 - 520 Ω m.

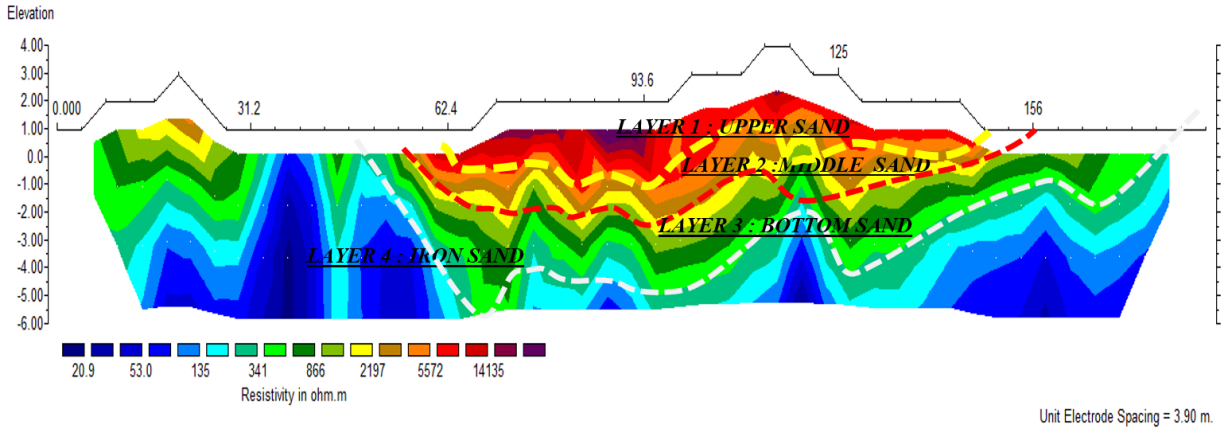

Figure 8. Resisitivity Inversion With Topography Data in Section 3

In this section (Figure 8), the upper sand area is less than the upper sand in sections 1 and 2. However, what's interesting about this section is that the organic material found only at a few electrode points has a much higher specific resistance than the previous section. Here there is sand with a mixture of organic materials with a higher concentration, resulting in a range of resistivity values greater than 14000 Ω m. The depth of this material is around 1 m with a length 11.7 m seen from the number of electrodes that pass through it. The range of resistivity values for this upper sand layer is 5572 – 14135 Ω m, indicated by red to purple colors.

The second layer in the form of sand with a mixture of gravel called the middle sand layer, indicated by yellow to orange color, has a resistivity value 1000 – 5572 Ω m. Based on the cross-sectional drawing above, the thickness of this sand layer is 2 m with a depth of 0.5 to 2 m from surface.

The layer of iron sand in this section is spread quite widely under the surface and there is also some that appears to the surface. Indicated by blue (iron sand) to green (bottom sand), the iron sand that appears is of low resistivity with a higher amount of Fe minerals.

The resistivity value of iron sand in this path ranges from 20.9 to 1000 Ω m

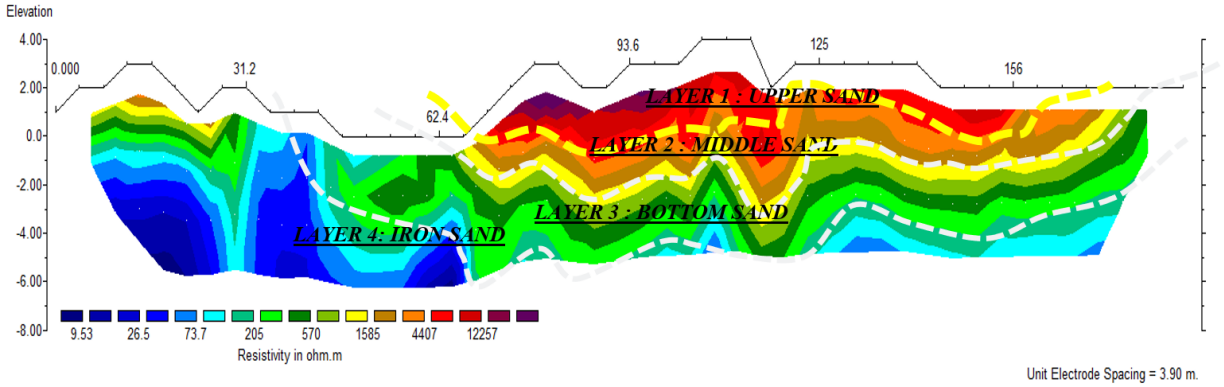

Figure 9. Resisitivity Inversion With Topography Data in Section 4

Similar to section 3, the upper sand layer of section 4 has little organic material compared to other upper sand layers (Figure 9). The concentration of organic material in section 4 is lower than in layer 3. However, in this layer, the sand which is the dominant material is more than the sand in the upper sand layer 3.

The highest resistance value is more than 12257 Ω m, the resistivity range of layer 1 is 5000 – 12257 Ω m as seen from the red – purple color. Its thickness is estimated to be around 1.5 m

The second layer in the form of sand with a mixture of gravel with a yellow to orange color is called the middle sand layer, has a resistivity value 1000 – 5000 Ω m. Based on the cross-sectional drawing above, the thickness of this sand layer is 2, m with a depth of 0 to 2 m from surface with a distribution length along 130 m.

The layer of iron sand (bottom sand and iron sand layer) on this section is also the same as the spread of iron sand on section 3, which is spread quite widely under the surface and some of it appears to the surface. The resistivity value of iron sand in this path ranges from 9.53 – 1000 Ω m. Where this value is the lowest among the previous 3 sections, so it can be interpreted that the quality / quantity is also better than the iron sand mineral of the previous 3 sections. The range of resistivity values of this iron sand layer is shown in blue to dark green.

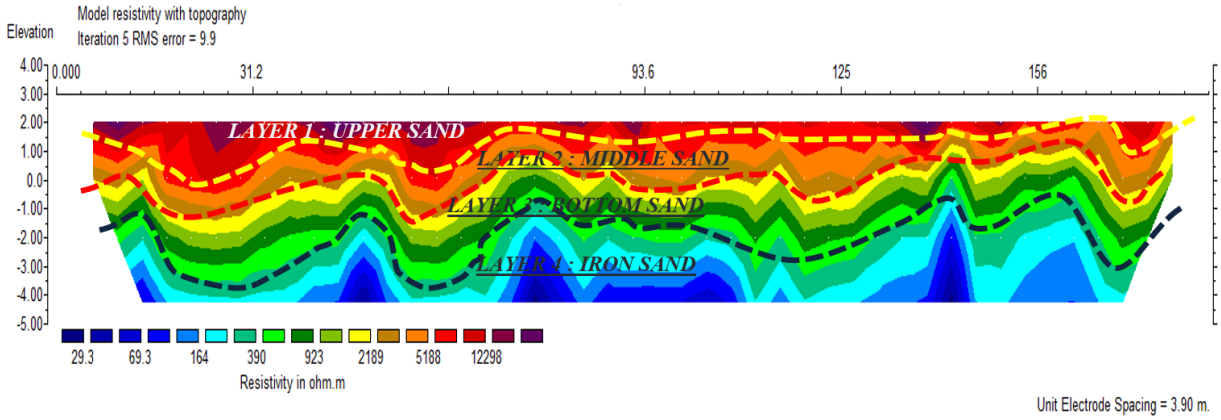

Figure 10. Resisitivity Inversion With Topography Data in Section 5

Section 5 in Figure 10 is a path that is made to intersect the previous path. The upper sand on this section also has a high specific resistance, which exceeds 12298 Ω m. The thickness of the upper sand layer has an average of 1 m, located at an elevation of 3 to 1 masl. The sand here also contains organic material with an amount less than paths 1 and 2, but in high concentrations. It is recorded that the resistivity values are red to purple with a range 5188 to 12298 Ω m.

The section area of 5 sand and gravel is spread almost evenly with a thickness 1-1.5 m, which is located at a depth of 1 m above sea level to 0.5 m below sea level. The resistivity range of this layer from 1000 to 5188 Ω m and is represented by yellow to orange color and is named middle sand layer. Iron sand is generally found at a depth of 2 – 4.5 m below sea level with an average thickness of 2.5 m. However, the resistivity value of path 5 is the highest compared to the resistivity of the previous 4 paths, which is 29.3 Ω m – 570 Ω m. Iron sand is indicated by blue to green color which is named bottom sand and iron sand layer.

Figure 11 and 12 below, are model of correlation of 5 sections of measurement. We can see the section point of section 1-4 that crossified by section 5. After correlated, it seems that iron sand located in SW direction or we can say that the iron sand is thicker to the shore.

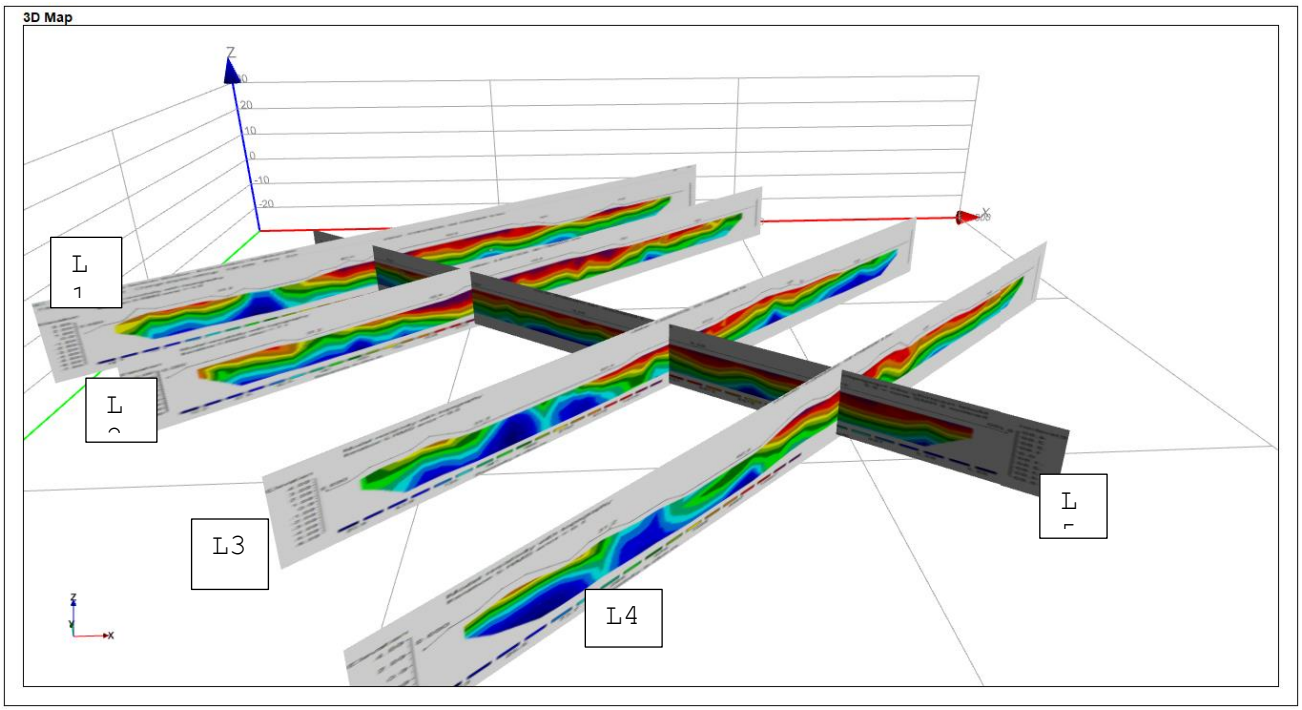

Figure 11. Correlation of 5 Sections in Study Area East Direction

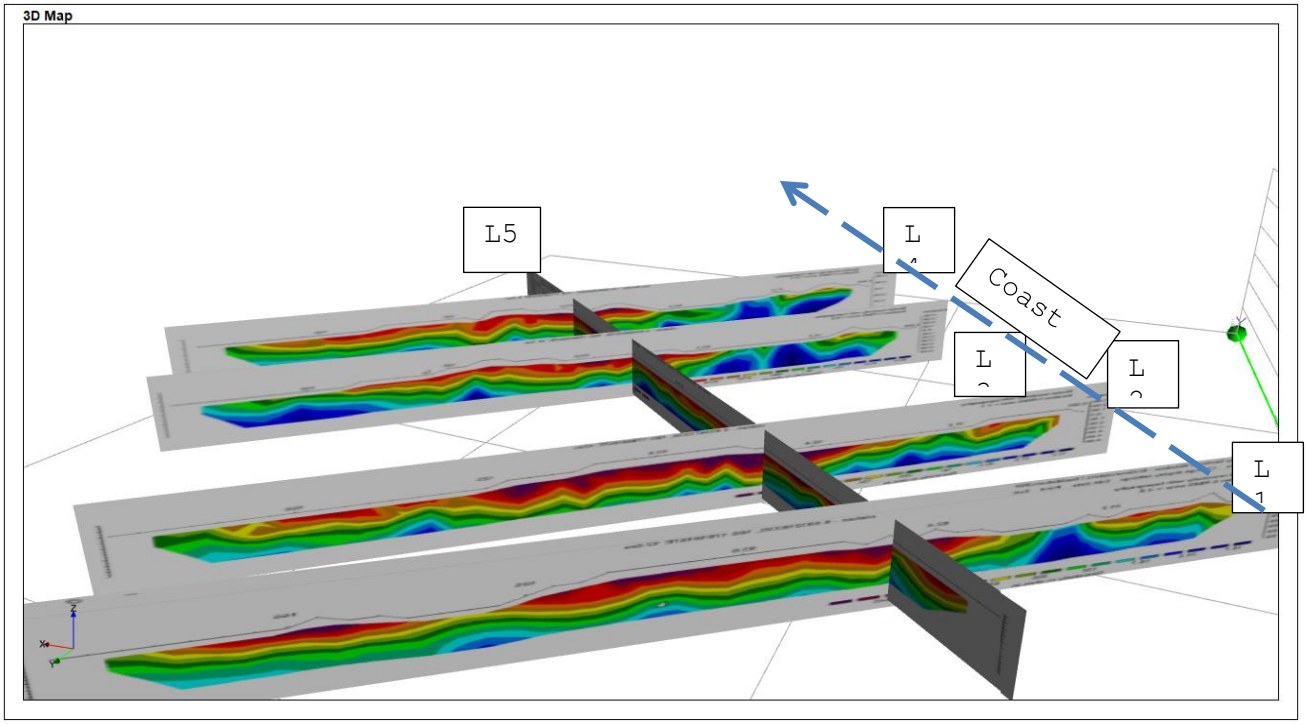

Figure 12. Correlation of 5 Sections in Study Area NW Direction

The Figure 13, 14, and 15 below show us how the 3d model of iron sand along with the lithology of the study area is. We can see that the SW direction has significant amount of iron sand.However, the

location doesn't suitable to be mined, and this happens because the folks around this area use this beach for living.

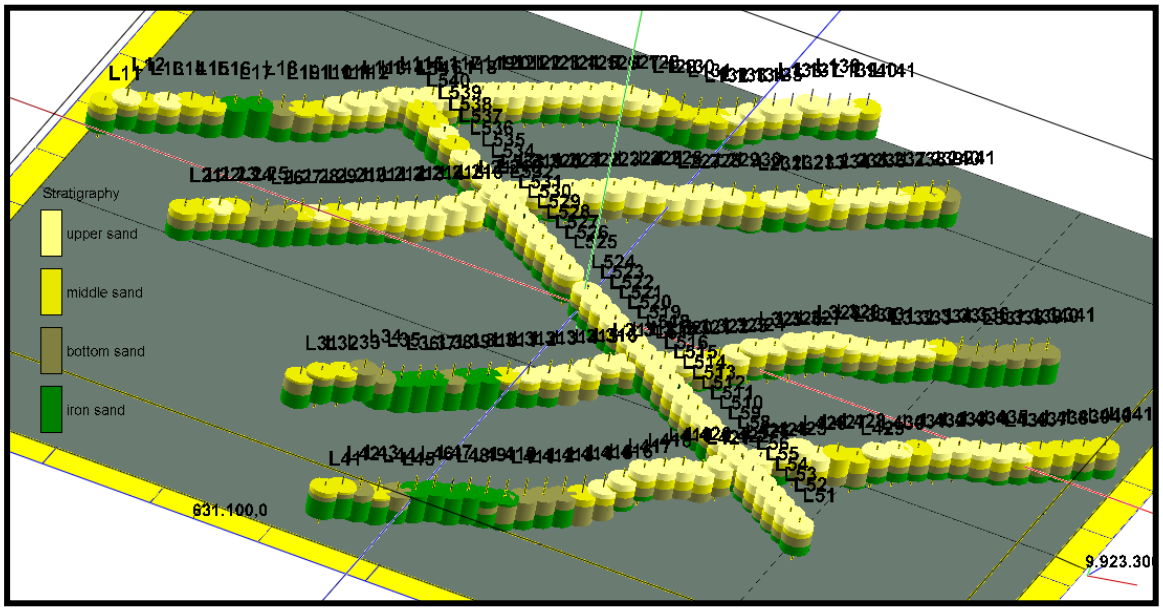

Figure 13. Dispersion and Lithology of Drill Logs in Research Area

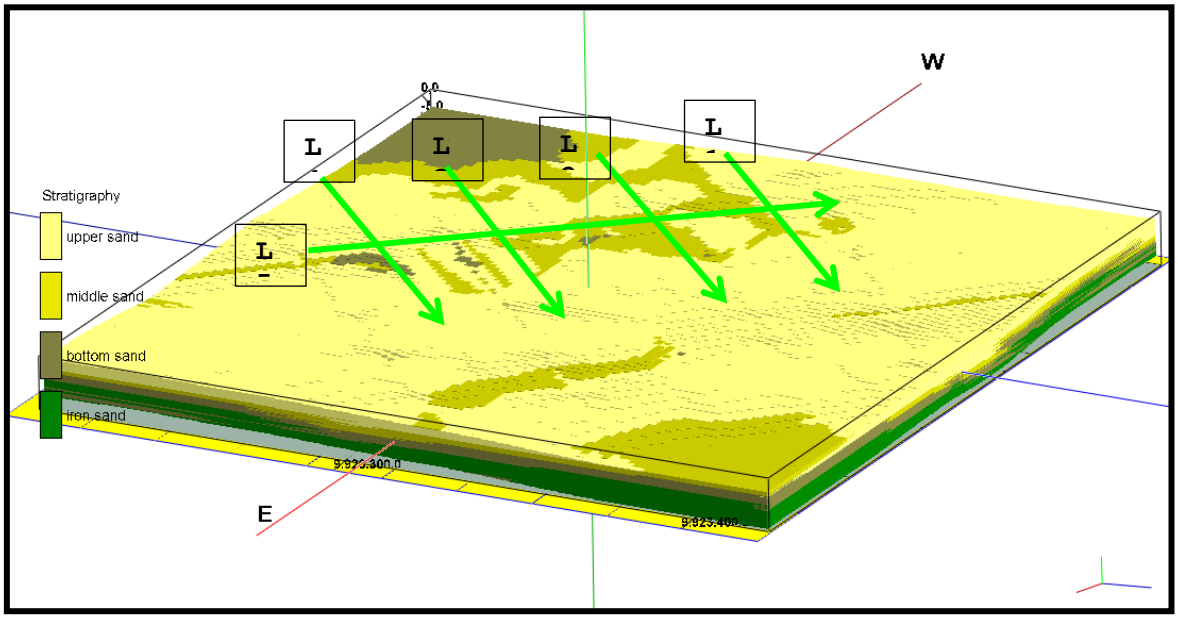

Figure 14. 3D Solid Model of Iron Sand in Study Area using RockWork Software

Thickness of iron sand in SW direction is from 0 to 6 meters as SW is the area with the highest content of iron sand (green). As for the sand, is the primary material in this area. If we compare this figure with geologic map in figure 4, we can see occurences and how the form of sedimentology in this Ulakan Tapakis. Iron sand is found thicker in shore line (thiner to the North or North-East).

This model is the same if we match with the correlated pseudosection above. The iron sand deposit is thicker to shore. The main cause of this situation is waves. Waves cause the sand particles dislodges as the sudden release of energy over a small area during the waves breaking the shore. The waves

approaching the shore in a different direction (opposite direction), so that it forms longshore current or littoral drift.

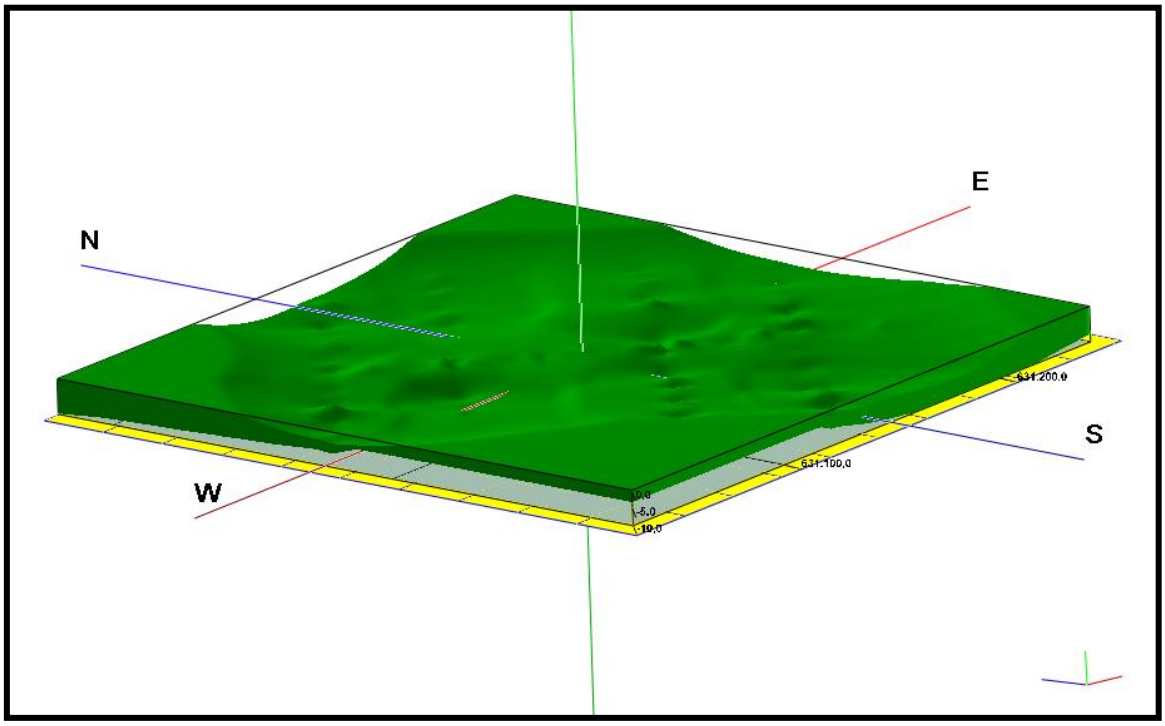

Figure 15. 3D Model of Iron Sand Layer Using Rockwork Software

6. Conclusions

This research provides the information of iron sand potential in Ulakan Tapakis, Padang Pariaman. Based on the discussion above, Ulakan Tapakis has 3 main components of alluvial deposits, namely a layer of top sand (upper sand), middle sand, and a layer of iron sand which is divided into 2 layers, namely the bottom sand and the iron sand layer which has a resistivity value ranging from 9.53 -14135 Ωm. These layers have different resistivity values depending on the constituent material.

For the iron sand carrier layer, the dominant layer is in the 4th layer, which is named the iron sand layer, followed by the bottom sand layer which contains silt material. This layer is represented by a blue to green color 9.53 – 1000 Ωm. Generally this layer is found at a depth of 0-6 meters below sea level. Its thickness ranges from 1 to 6 meters.

Acknowledgments

The authors would like to thank Lembaga Penelitian dan Pengabdian Masyarakat Universitas Negeri Padang for funding this work with a contract number : 892/UN35.13/LT/2021.

References

[1] Razi, P., Sumantyo, J. T. S., Ali, S., Aminuddin, J., Kurniawan, F., Putra, R. R., & Octova, A. (2021, April). 3D modelling using structure from motion technique for land observation in Kelok 9 flyover. In Journal of Physics: Conference Series (Vol. 1876, No. 1, p. 012026). IOP Publishing.

[2] Andani, Y., & Octova, A. (2020). EKSPLORASI PASIR BESI KAWASAN PASIA PANEH NAGARI TIKU SELATAN KECAMATAN TANJUNG MUTIARA SEBAGAI BAHAN BAKU INDUSTRI DI SUMATERA BARAT. Bina Tambang, 5(3), 88-101.

[3] Prabowo, H. (2020, March). Genes and physical properties of iron sand from Kinali Pasaman. In Journal of Physics: Conference Series (Vol. 1481, No. 1, p. 012015). IOP Publishing.

[4] de Jong, S. M., Heijenk, R. A., Nijland, W., & van der Meijde, M. (2020). Monitoring soil moisture dynamics using electrical resistivity tomography under homogeneous field conditions. Sensors, 20(18), 5313.
[5] Octova, A., Muji, A. S., Raeis, M., & Putra, R. R. (2019, April). Identification of Aquifer using Geoelectrical Resistivity Method with Schlumberger Array in Koto Panjang Area, Nagari Tigo Jangko, Lintau Buo Sub-District, Tanah Datar Regency. In Journal of Physics: Conference Series (Vol. 1185, No. 1, p. 012009). IOP Publishing.
[6] Loke, M. H. (2004). Tutorial: 2-D and 3-D electrical imaging surveys.
[7] Telford, W. M., Geldart, L. P., & Sheriff, K. D. (1976). Applied geophysics.,(Cambridge University Press: Cambridge, UK).
[8] Mufit, F., Fadhillah, H. A., & Bijaksana, S. (2006). Kajian tentang Sifat Magnetik Pasir Besi dari Pantai Sunur Pariaman Sumatera Barat. Jurnal Geofisika, Bandung.
[9] Budiman, A. (2014). Pemetaan Persentase Kandungan Dan Nilai Suseptibilitas Mineral Magnetik Pasir Besi Pantai Sunur Kabupaten Padang Pariaman Sumatera Barat. Jurnal Fisika Unand, 3(4), 242-248.
[10] Prabowo, H., & Sumarya, S. (2017). Investigation of Chemical Feasibility and Distribution of Iron Sand Reserve Regional Area of Agam District for Cement Eaw Material in PT. Semen Padang.
[11] Octova, A., & Yulhendra, D. (2017). Iron ore deposits model using geoelectrical resistivity method with dipole-dipole array. In MATEC web of conferences (Vol. 101, p. 04017). EDP Sciences.
[12] Reynolds, J. M. (2011). An introduction to applied and environmental geophysics. John Wiley & Sons.
[13] Rianna, M., Sembiring, T., Situmorang, M., Kurniawan, C., Setiadi, E. A., Tetuko, A. P., ... & Sebayang, P. (2018). Characterization of Natural Iron Sand From Kata Beach, West Sumatra With High Energy Milling (Hem). Jurnal Natural, 18(2), 97-100.